Insulator Recognition and Fault Detection Using Deep Learning Approach

Eldad Antwi-Bekoe[1,2], Qiugang Zhan[1], Xiurui Xie[1,3], Guisong Liu[1,4]

[1] University of Electronic Science and Technology of China, Chengdu, 611731, China.

[2] University of Education Winneba, P. O. Box 1277, Kumasi, Ghana.

[3] Agency for Science, Technology and Research, Singapore.

[4] UESTC. Zhongshan, 528400, China

eabekoe@uew.edu.gh, zhanqg@foxmail.com, xiexiurui@126.com, lgs@uestc.edu.cn

ABSTRACT. Uninterrupted power supply to electric power consumers has increasingly become a global necessity. Monitoring the health of distribution network is crucial to provide quality service. Traditional monitoring methods based on on-site patrols to detect faults have increasingly become labor-intensive and time-consuming, raising demand for new and more efficient techniques. To address this issue, we propose faster-RCNN by MXNet for both detection and classification tasks. We utilize convolutional neural network (CNN) for detecting and classifying both insulator components and faulty insulator discs from images captured on overhead electric power transmission systems. Using a dataset of images acquired through UAV (unmanned aerial vehicle) captures, detection and classification is dealt with by dividing the picture content of the training set into three classes: background, insulator and the defective part of insulator. We achieve target insulator recognition and positioning with impressive precision compared to other traditional technologies. Our work could have practical integrated implementation solutions for automated inspection of overhead transmission power line insulators. The code used can be found at https://github.com/QgZhan/Insulator-Defect-Detection.

Keywords. Insulator recognition; Faster R-CNN; Power Systems; outlier detection

1. Introduction

Power systems strive to ensure high availability and undisrupted flow of Power. However, adverse conditions on power distribution lines occur which could result in outage times and also present hazardous conditions to humans and the environment. Moreover, prolonged changes in climatic conditions, exceeding a certain voltage capacity, vandalism and "spontaneous shattering" [1] of toughened glass shell can reduce the strength of the insulators which could possibly cause of an outage. Other types of insulator defect possibilities are cited in [1]. One major goal of electric utilities is to drop maintenance costs by adopting appropriate inspection strategy to pinpoint, follow-up and to repair any significant failures at the earliest possible stage [2] Computer vision technology can be utilized to process and extract insulators from the video/image [3] and also to pinpoint defects [4] on the insulators. Images of the insulators taken from the power distribution lines using high quality video cameras, at regular time intervals can be sent to the control room using remote terminal units (RTUs) [5] or UAVs [6] for further processing. This work aims at extracting by localizing and detecting the

insulator component of input images, and classifying insulator units (as normal or defective) from captured images of UAV photographs utilizing faster R-CNN technique. Most existing work have focused on hand crafted feature extraction methods [7] [8] [9]which are influenced by lots of factors. These factors finally result in poor generalization.

The main contribution of our work is the application of relatively new technology of deep learning by utilizing CNN to (i) recognize power tower insulators from UAV images (ii) to detect outliers of insulator units on power towers, which to the best of our knowledge has not been extensively explored in the field of object detection. We also note that most previous efforts have focused on only either both insulator location and classification alone or on only fault detection on insulator component.

The rest of the paper is organized as follows; we present some research trend analysis in section 2, then the Faster R-CNN training framework, architecture used, followed by relevant training procedures by describing feature extraction and image processing, detection and classification essentials in section 3. Next, we present some details of our experiment, classification framework and the detection procedure of our study. We present results and evaluation of this study in section 4. We conclude our work and present scope for future research in the last section.

2. Related work

Due to their ability to learn discriminative features from raw data inputs (e.g., image pixels), CNNs have recently gained impressive performance in a number of visual recognition systems [10]; notably in classification [11] and detection [12] Object recognition pipelines have typically involved feature extraction, object detection, localization and classification stages. Traditional insulator detection methods employed hand engineered feature extraction on images as an initial pre- processing step [10].

Recent developments have explored image processing techniques followed by machine learning as a feasible option for real time detection implementations. Pattern Histogram Fourier features (LBP-HF) [7]is a rotation invariant image descriptor computed from discrete Fourier transforms of local binary pattern (LBP) histograms where Insulators are extracted from captured images using k-means clustering, SVM is used as the classifier. A rotation invariant insulator detection approach is introduced in [8] where sliding window based local directional pattern (LDP) feature is extracted from the image and SVM is used for classing each of those sliding windows. Most of these hand-crafted local features including LBP [7] HOG [9] deformable part models (DPM) [9] etc. are very powerful, they can hardly capture any information other than what have been defined by prior knowledge [13].

Traditional approaches have primarily addressed feature extraction problem by using a single type of feature such as color feature, texture feature, or shape feature. Guoxiong et al [14] argues that a single type of feature usually leads to poor classification rates and missed detection in identifying insulators. Fault detection algorithm that exploits an adaptive learning scheme by combining color and the gradient features to locate the insulator, is presented in [15].

Insulator detection and localization using a sliding window scheme with the aid of Non Maximum Suppression (NMS) algorithm and line fitting method is studied in [16] The methodology effectively localizes the insulator with a better precision compared to other traditional methods in [9] [17]. However, this study is limited to only insulator detection and not fault detection. More traditional insulator recognition pipelines compute hand-engineered features depend on color features and other geometric features. These methods would be influenced by lots of factors including illumination and background in result, getting poor generalization ability [16].

Propelled by GPU implementations which efficiently perform massive parallel computations required for learning and inference in large CNNs, these networks have become the most accurate method for generic object classification [8]. Our work is inspired by the R-CNN method in [18] which effectively extracts features from a deep CNN in a region proposal framework to achieve remarkable object detection results on the PASCAL VOC dataset. What differs from [18] is that our implementation uses apache MXNet framework [19]. Secondly, we use a different (private) dataset of UAV captured images of insulators. We also modify the programming code to better fit our model.

We note that this paper does not focus on well-being analysis that provides a means to perceive the state of health of an insulator whether it is in a good condition or in a state of risk of damage [4] [20] [21] [22] [23]. We therefore define fault (or disc defect) as a missing insulator unit rather than as any other abnormal condition of the insulator which results in a reduced performance, or produces disruption or failure in power transmission.

3. Framework of architecture

The faster RCNN used in this work is based on original Faster RCNN as described in [18]. The faster RCNN detection system is composed of four modules. The first module, the base network is a deep CNN that generates feature map of input image by using ReLU and max pooling. In the second module, a region proposal network (RPN) generates region proposals. Region of Interest pooling (RoI pooling) uses feature maps and proposals to generate proposal feature maps in the third module.
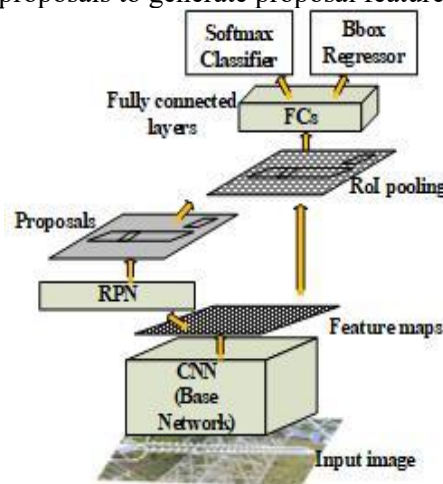

Figure 1. Unified Faster R-CNN end-to-end training architecture

Lastly, the generated proposal features are forwarded to two separate fully connected layers and a softmax classifier that classifies them into the respective classes. Moreover, bounding box regression is used to regulate the position of predicted bounding box according to the predicted class. The entire framework embodies a single, unified network for object detection (Figure 1). In the next subsections we describe our dataset, then we discuss detailed role played by each module within the entire architecture.

3.1. Dataset

1600 images are collected using UAV equipped with G15 Canon camera in various environments that include forests, shrubby vegetation, mountainous terrain, etc. The sample data contains images captured from different distances, angles and different gradients of illuminated backgrounds, as well as different weather conditions suitable for data collection. Our dataset also contains large images with high resolution (5,472 X 3,648 pixels). High resolution images with large surface area situating small insulator(s) and defective disc(s) as targets for detection also add some difficulties for object detection accuracy.

In the experiments, we divide the sample into two parts: the training set that contains 1500 samples is the insulator, 300 of them contained defective insulators. The test dataset of 100 containing 50 defective insulators. The original image sizes were narrowed down to 1400*800 to enhance the efficiency of feature learning [8] and also to facilitate the training process.

3.2. Faster R-CNN training

The original work in [18] discusses the three different approaches by which Faster R-CNN can be trained. Our work implements the joint training approach because experiments in [18] proved that doing end-to-end, merged training is faster and leads to better results. The training set is denoted as X = $\{(x^{(1)}, y^{(1)}), (x^{(2)}, y^{(2)}),\ldots, (x^{(m)}, y^{(m)})$, with $x^{(i)}$ as input image having a corresponding label $y^{(i)}$. A

supervised learning representation learns a mapping function Y = F(X|θ) or the posterior distribution P(Y|X).

3.3. Classification framework

In the final stage proposals are classified for each output box by utilizing softmax with a category label of a non-defective or defective insulator. Each of the different object proposals is forward pass through two fully connected layers. This stage also implements a better adjustment of the proposed bounding box using bounding box regression for a predicted class. We define the combined training set loss for the network as:

$$L(p_i, t_i) = \frac{1}{N_{cls}} \sum_i L_{cls}(p_i, \hat{y}) + \frac{\lambda}{N_{reg}} \sum_i \hat{y} L_{reg}(t_i, t_i^*). \tag{1}$$

where i represents the index of an anchor, pi the predicted probability of i, $\hat{y}$ the ground-truth label and. ti the vector representing the coordinates of the predicted bounding box, ti* the ground-truth box associated with a positive anchor and λ the balancing parameter. Lcls is log loss over the two classes (defective or non-defective) and Lreg the regression loss. In this work we use $L_{reg}(t_i, t_i^*)$ = R(ti – ti*) where R is the robust loss function (smooth L1) defined in [24]. L_{reg} and L_{cls} are normalized by the mini-batch size Ncls (256) and by the number of anchor location Nreg (~2400). For bounding box regression, we adopt the parameterizations of the four coordinates following [25].

3.4. Detection procedure

1) RPN Proposals: During detection, the RPN component serves as the 'attention' of the unified network [18] and instructs the detection module (Fast R-CNN) [24] where to look. RPN predicts the possibility that an anchor is a background or foreground (object). It simply produces proposals or boxes that will be eventually examined by a classifier and regressor in the detection module to confirm the occurrence of objects. We implement a 3 X 3 sliding window scheme to predict a set of dense candidate regions or "proposals" of varying sizes; three scales (8, 16, 32) and three aspect ratios (1:1, 1:2, 2:1). This is attended to by the Fast R-CNN detector which eventually refines the proposals by applying regression coefficients generated by the RPN to ultimately improve detection accuracy.

RPN first takes feature inputs generated from the "conv5" layer of the deep CNN (VGG-16). It slides 3 X 3 filters over the feature maps to make class-agnostic region proposals using VGG network. We note that RPN stage of Faster R-CNN model is a two-stage process comprising class-agnostic proposals and class-specific detections. We set the top N proposals during training to 12,000 and reduce it to 2000. During testing, we set the top N proposals to 6000 and eventually reduce it to 300. The output for the first stage of RPN proposals is multiple candidate boxes of different sizes, generated around insulator ground truth box (Figure 2a). Generally, Non-maxima suppression (NMS) is used to suppress bounding boxes that have a significant overlap with each other. The version of NMS we use does not merge ROIs but rather tries to identify which ROIs best cover the actual locations of an object, then we discard by manually deleting all other ROIs.

We do this by selecting bounding box proposals with highest foreground scores to add to the final output list. NMS does not harm the ultimate detection accuracy, but substantially reduces the number of proposals [18] by dropping the proposals which do not meet a certain threshold for intersection of union (IoU); in our case ≥ 0.7 for the same class set. We delete predicted boxes that do not have intersection with any ground truth or boxes that do not overlap with our object of interest such that only a single box is retained to avoid redundancy (Figure 2b). This means boxes labelled as background aren't included in the regression, as we don't have ground-truth boxes for them. After applying NMS, we keep the top N = 2000, sorted by score.

2) Region of Interest Pooling: At the second stage is a RoI layer that undertakes RoI pooling by taking two inputs; (a) A fixed-size feature map obtained from the base network imbedding several convolutions and max pooling layers. (b) An N × 5 matrix representing multiple candidate proposals or regions of interests, where N indicates the number of RoIs. The other fields of the matrix contain the coordinates of the RoIs and the index of the input image. Using max pooling, RoI layer warps all

ROIs into a fixed size vector of $7 \times 7 \times 512$ dimension in one single layer. The result of RoI pooling is that, multiple rectangular proposals ends up mapping to corresponding feature maps of a particular fixed size.

In summary, RPN simply produces proposals or boxes that will eventually be examined by a classifier and regressor in the detection module to confirm the occurrence of objects.
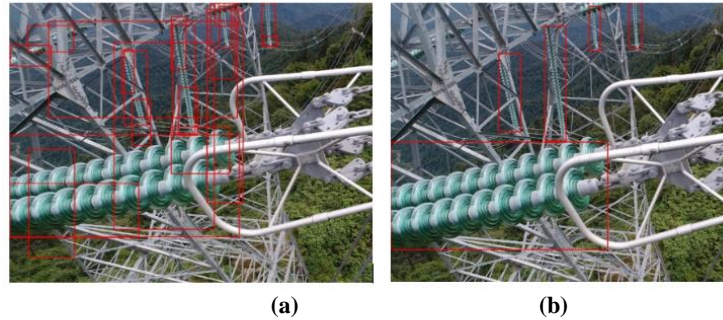

(a)   **(b)**

Figure 2. (a) Predicted proposals after faster R-CNN training. (b) Result of insulator target after NMS suppression. An objectness score threshold of 0.7 is used to display these images.
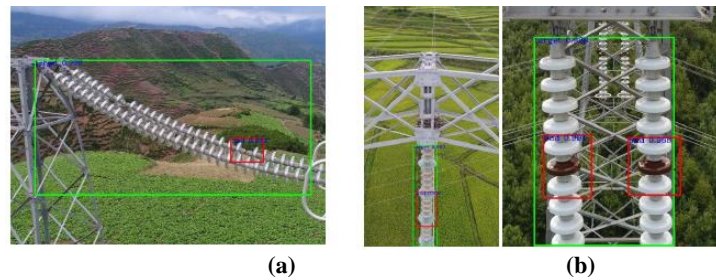

(a)   **(b)**

Figure 3. (a) Insulator target with correctly predicted defective unit and a missed prediction. (b) Insulator targets showing incorrectly predicted defective units.

3) Classification: The final output of the VGG network is a transformed RoI feature vector, a 512-dimensional vector, which we feed into 2 fully connected layers to predict a boundary box and 2 objectness scores using a regressor and softmax classifier respectively. The classifier predicts 2 possible classes: one for the "insulator target object" category and one for the "defective disc" category. RPN makes η guesses for each location of the feature maps, which means RPN outputs $4 \times η$ coordinates and $2 \times η$ scores per location. We also perform non-maximum suppression independently for each class using the algorithm and settings from R-CNN [26].

Algorithm 1 NMS Algorithm for Bounding box regression

Input: $B = \{b_1, b_2, \ldots, b_n\}, S = \{S_1, S_2, \ldots, S_n\}, N_t$
  1: Where B is the list of initial detection boxes. S contains corresponding detection scores, N_t is the NMS threshold
Output: D, S
  2: $D \leftarrow \{\}$
  3: **while** $B \neq empty$ **do**
  4:     $m \leftarrow argmax(S)$
  5:     $M \leftarrow b_m$
  6:     $D \leftarrow D \cup M$
  7:     $B \leftarrow B - M$
  8:     **for** b_i in B **do**
  9:       **if** $IoU(M, b_i) \geq N_t$ **then**
10:         $B \leftarrow B - b_i$
11:         $S \leftarrow S - s_i$
12:       **end if**
13:     **end for**
14: **end while**

Figure 4 shows a plot of the training accuracy of our model. From the plot, our model's learning accuracy improves over time as the number of epochs increases. This is reflective on the training log loss plot as shown in Figure 6. As expected, the loss minimizes as the number of epochs increases indicating that the model learns better over time; a pointer to improved accuracy in classification performance of our model. The training L1 loss plot shown in Figure 5 also confirms improvement in learning, as error value of the difference between true values and predicted values minimizes with increase in number of epochs.

4. Results and evaluation

4.1. Experimental set up

During the training phase, we use VGG-16 architecture network [26] to train the detection model. The base network, a VGG-16 network takes the input image of sizes cropped down to 1400*800. Training is done on a Tesla K80 GPU. Learning was stopped after 10 epochs because we found it the best fit for our model, beyond which we found no improvements. Manually restricting the epoch to this number in our work is also key to avoid overfitting. We use a momentum of 0.9. We start with a base learning rate of 0.001 and gradually decrease it to 0.0001 after 59 iterations. We follow other implementation details as defined in [18].

To the best of our knowledge, there is currently no publicly available dataset for insulator detection or insulator fault detection to date. We deploy our own private evaluation set. For the evaluation of the insulator (or defective disc) detection, to the best of our knowledge, there hasn't been any published work that has employed any standard evaluation metrics which could be referenced as a baseline.

Classification and detection results are evaluated based on the true positive rate (TPR) and Precision of prediction by our model. Here, TPR may be defined as the fraction of correctly identified insulators for the target category or as the fraction of correctly identified defective discs for the defective disc category; precision, a measure of prediction accuracy by our model.

4.2. Sensitivities to Hyper-parameters

Table 1 shows the detection results for different anchor settings on our test set. We note that 94.1% and 83.7% TPR detection rates were achieved on our test set using an anchor settings of 1 scale (with 3 aspect ratio) and 3 scales (with 1 aspect ratio) for insulator target and defective disc respectively as shown in Table 2. This represents the highest TPR rates for insulator and defective disc detection. This proves that considering anchors of multiple sizes as the regression references could be an effective solution.

Using one scale with three aspect ratios (94.1% TPR rate) is as good as using three scale with three aspect ratio settings (94.0% TPR rate) on this dataset for target insulator detection. This is a possible indication that scales and aspect ratios are not linked dimensions to influence insulator target detection accuracy.
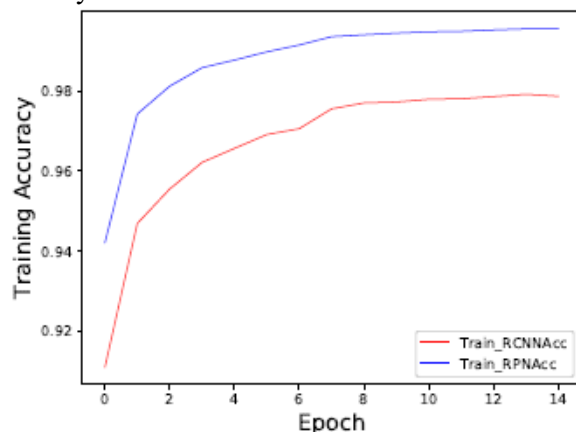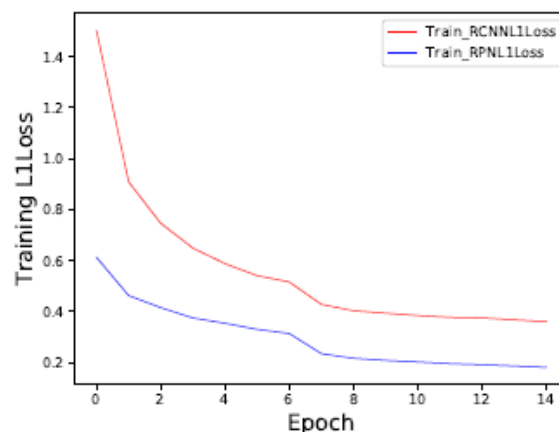

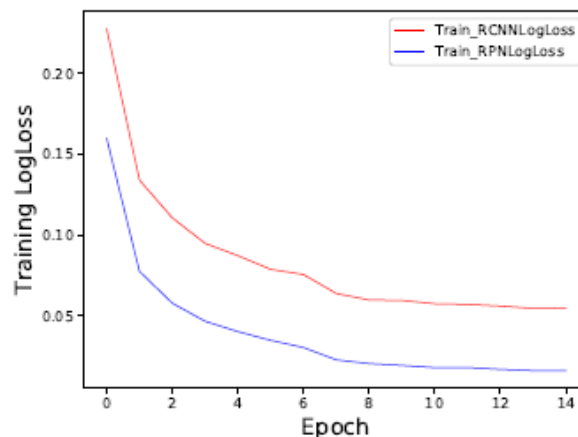**Figure 4.** Training Accuracy   **Figure 5**. Train L1 Loss

Figure 6. Train Log Loss

Table 1. Detection Results for Different Settings of Anchors on Our Test Set Using Faster R-CNN.

Settings	Anchor Scales	Aspect Ratios	Insulator Target			Defective Discs		
			TP	Miss Rate	FD	TP	Miss Rate	FD
1 Scale, 1 Ratio	8	1:1	91	7	80	35	16	1
	16	1:1	101	8	65	5	47	0
1 Scale, 3 Ratio	8	[2:1, 1:1, 1:2]	**96**	**6**	**81**	40	9	12
	16	[2:1, 1:1, 1:2]	92	6	84	10	41	3
3 Scale, 1 Ratio	[8, 16, 32]	1:1	91	10	83	**41**	**8**	**4**
3 Scale, 3 Ratio	[8, 16, 32]	[2:1, 1:1, 1:2]	94	6	81	39	11	5

Table 2. Average Classification Rates Based on TP Obtained Using Faster R-CNN Detection Module at Different Anchor Settings.

Settings	Anchor Scales	Aspect Ratios	Insulator Target	Defective Discs
			TPR (%)	TPR (%)
1 Scale, 1 Ratio	8	1:1	92.9	68.6
	16	1:1	92.7	9.6
1 Scale, 3 Ratio	8	[2:1, 1:1, 1:2]	**94.1**	81.6
	16	[2:1, 1:1, 1:2]	93.9	19.6
3 Scale, 1 Ratio	[8, 16, 32]	1:1	90.1	**83.7**
3 Scale, 3 Ratio	[8, 16, 32]	[2:1, 1:1, 1:2]	94.0	78.0

Table 3. Classification Accuracy Determined by Our Model

	Insulator Target		Defective Discs	
	Ratio	%	Ratio	%
TP	165/169	97.6	41/44	93.2
FDR[1]	11/176	6.2	9/53	16.9
Miss Rate	4/169	2.3	3/44	6.8
Precision	-	**93.75**	-	**82.0**

[1] – False Discovery Rate

4.3. Challenges

The relatively higher miss rate for the defective insulator unit detection task could possibly be due to (a) Limited number of defective insulator training set examples necessary to improve the feature learning representation. (b) The presence of overlapping views among insulator discs or an adjacent disc in a photographic image. (c) micro-views of defective insulator discs as a result of photographic distances of some insulator images.

Some functional insulator discs were wrongly classified as defective insulator discs (Figure 3b). Most of these were typically, replacement defective insulator discs that showed either some structural difference or color difference from the other discs that makes up the whole insulator component. This is also further proof that the model is able to identify minimal changes in insulator structure during object detection.

5. Conclusion

In this paper, we approach the detection of the insulator component and the defective part of the insulator (outlier) of power line transmission systems by utilizing convolutional neural network in Faster-RCNN model. By utilizing a sliding window scheme, the RPN component of the Faster R-CNN serves as the 'attention' of the unified network and instructs a detection module where to focus to improve detection accuracy. Our model also demonstrates high robustness by detecting target insulators and outliers from images taken from various distances, angles and background. We achieve precision of 93.75% and 82.0% (Table 3) on insulator component detection and defective insulator unit detection tasks respectively. The results achieved with this work is a promising feat for object detection in computer vision field, and good generalization with a large-scale dataset is expected. Future work considerations will involve combining transfer learning with spiking neural network to improve detection accuracy of target insulator and defective insulator units.

References

[1]   Gorur, Ravi. S. Failure modes of porcelain and toughened glass suspension insulators. (USA, Annapolis 2011), 221-225.

[2]   Prasad, P. Surya and Rao, B. Prabhakara. Review on Machine Vision based Insulator Inspection Systems for Power Distribution. *JOURNAL OF Engineering Science and Technology Review*, 9, 5 (2016), 135-141.

[3]   Wang, Xian and Zhang, Youmin. Insulator identification from aerial images using Support Vector Machine with background suppression. *2016 International Conference on Unmanned Aircraft Systems (ICUAS)* (2016), 892-897.

[4]   Murthy, Velaga Sreerama, Kumar, Mohanta Dusmanta, and Gupta, Sumit. Power system insulator condition monitoring automation using mean shift tracker-FIS combined approach. *International Journal of Computer Aided Engineering and Technology*, 5, 1 (2013), 1-19.

[5]   Avidar, Baruch. Electronic airborne inspection method for overhead transmission power-lines. (Las Vegas 1993), 89-93.

[6]   Katrasnik, Jaka, Pernus, Franjo, and Likar, Bostjan. A survey of mobile robots for distribution powerline inspection. IEEE Transactions on Power Delivery. *IEEE Transactions on Power Delivery*, 25, 1 (2010), 485-493.

[7]   Prasad, P. Surya and Rao, B. Prabhakara. LBP-HF features and machine learning applied for automated monitoring of insulators for overhead power distribution lines. (India 2016), 808-812.

[8]   Jabid, Taskeed and Uddin, Md. Zia. Rotation invariant power line insulator detection using local directional pattern and support vector machine. (Dhaka 2016), 1-4.

[9]   Felzenszwalb, P. F., Girshick, R. B., McAllester, D., and Ramanan, D. Object Detection with Discriminatively Trained Part-Based Models. *IEEE Transactions on Pattern Analysis and Machine Intelligence*, 9, 32 (2010), 1627-1645.

[10]   Zhang, Ning, Donahue, Jeff, Girshick, Ross, and Darrell, Trevor. Part-Based R-CNNs for Fine-Grained Category Detection. (Zurich 2014), Springer, 834-849.

[11]   Krizhevsky, Alex, Ilya, Sutskever, and Hinton, Geoffrey E. ImageNet Classification with Deep Convolutional Neural Networks. *Neural Information Processing Systems*, 1 (2012), 1106–1114.

[12]   Sermanet, Pierre, Eigen, David, Zhang, Xiang, Mathieu, Michael, Fergus, Rob, and LeCun, Yann. OverFeat: Integrated Recognition, Localization and Detection using Convolutional

Networks. *ArXiv e-prints* (Dec. 2013).

[13]   Zuo, Zhen, Wang, Gang, Shuai, Bing, Zhao, Lifan, Yang, Qingxiong, and Jiang, Xudong. Learning Discriminative and Shareable Features for Scene Classification. (2014), Springer International Publishing, 552-568.

[14]   Guoxiong, Hu, Zhong, Yang, Maohu, Zhu, Li, Huang, and Naixue, Xiong. Automatic classification of insulator by combining k-nearest neighbor algorithm with multi-type feature for the Internet of Things. *EURASIP Journal on Wireless Communications and Networking*, 2018, 1 (July 16, 2018), 117.

[15]   Zhai, Yongjie, Wang, Di, Zhang, Muliu, Wang, Jiarong, and Guo, Feng. Fault detection of insulator based on saliency and adaptive morphology. *Multimedia Tools and Applications*, 76, 9 (May 01, 2017), 12051-12064.

[16]   Liu, Yue, Yong, Jun, and Liu, Liang. The method of insulator recognition based on deep learning. (Jinan 2016).

[17]   Lazebnik, S., Schmid, C., and Ponce, J. Categories, Beyond Bags of Features: Spatial Pyramid Matching for Recognizing Natural Scene. (New York, NY, USA 2006), 2169-2178.

[18]   Ren, Shaoqing, He, Kaiming, Girshick, Ross, and Sun, Jian. Faster R-CNN: Towards Real-Time Object Detection with Region Proposal Networks. *IEEE Transactions on Pattern Analysis and Machine Intelligence*, 39, 6 (2017), 1137-1149.

[19]   Chen, Tianqi, Li, Mu, Li, Yutian et al. MXNet: A Flexible and Efficient Machine Learning Library for Heterogeneous Distributed Systems. *Neural Information Processing Systems, Workshop on Machine Learning Systems* (2016).

[20]   Guo, Li, Liao, Yu, Yao, Hongying, Chen, Jinhao, and Wang, Manran. An Electrical Insulator Defects Detection Method Combined Human Receptive Field Model. *Journal of Control Science and Engineering*, 2018 (2018).

[21]   Murthy, Velaga Sreerama, Gupta, Sumit, and Mohanta, D. K. Digital image processing approach using combined wavelet hidden markov model for well-being analysis of insulators. *IET Image Processing*, 5, 2 (2011), 171-183.

[22]   Murthy, Velaga Sreerama, Tarakanath, K., Mohanta, D. K., and Gupta, Sumit. Insulator condition analysis for overhead distribution lines using combined wavelet support vector machine. *IEEE Transactions on Dielectrics and Electrical Insulation*, 17, 1 (2010), 89-99.

[23]   Reddy, M. Jaya Bharata, Karthik Chandra, B., and Mohanta, D. K. Condition Monitoring of 11 kV Distribution System Insulators Incorporating Complex Imagery Using Combined DOST-SVM. *IEEE Transactions on Dielectrics and Electrical Insulation*, 20, 2 (2013), 664-674.

[24]   Girshick, Ross B. Fast R-CNN. (Santiago 2015), IEEE.

[25]   Girshick, R., Donahue, J., Darrell, T., and Malik, J. Rich Feature Hierarchies for Accurate Object Detection and Semantic Segmentation. (USA, Columbus 2014), 580-587.

[26]   Simonyan, Karen and Zisserman, Andrew. Very deep convolutional networks for large-scale image recognition. *CoRR*, abs/1409.1556 (2014).